Atmos. Chem. Phys. Discuss., 8, 5629–5681, 2008
www.atmos-chem-phys-discuss.net/8/5629/2008/
© Author(s) 2008. This work is distributed under
the Creative Commons Attribution 3.0 License.

Atmospheric Chemistry and Physics Discussions

The influence of chemical composition and mixing state of Los Angeles urban aerosol on CCN number and cloud properties

M. J. Cubison[1], B. Ervens[2,3], G. Feingold[3], K. S. Docherty[1], I. M. Ulbrich[1,4], L. Shields[5], K. Prather[5], S. Hering[6], and J. L. Jimenez[1,4]

[1]Cooperative Institute for Research in the Environmental Sciences (CIRES), University of Colorado, Boulder, CO, USA
[2]Atmospheric Science Department, Colorado State University, Fort Collins, CO, USA
[3]NOAA Earth System Laboratory, Boulder, CO, USA
[4]Dept. of Chemistry and Biochemistry, University of Colorado, Boulder, CO, USA
[5]University of California at San Diego, CA, USA
[6]Aerosol Dynamics, Inc., Berkeley, CA, USA

Received: 31 January 2008 – Accepted: 4 February 2008 – Published: 18 March 2008

Correspondence to: J. L. Jimenez (jose.jimenez@colorado.edu)

Published by Copernicus Publications on behalf of the European Geosciences Union.

Abstract

The relationship between cloud condensation nuclei (CCN) number and the physical and chemical properties of the atmospheric aerosol distribution is explored for a polluted urban data set from the Study of Organic Aerosols at Riverside I (SOAR-1) campaign conducted at Riverside, California, USA during summer 2005. The mixing state and, to a lesser degree, the average chemical composition are shown to be important parameters in determining the activation properties of those particles around the critical activation diameters for atmospherically-realistic supersaturation values. Closure between predictions and measurements of CCN number at several supersaturations is attempted by modeling a number of aerosol chemical composition and mixing state schemes of increasing complexity. It is shown that a realistic treatment of the state of mixing of the urban aerosol distribution is critical in order to eliminate model bias. Fresh emissions such as elemental carbon and small organic particles must be treated as non-activating and explicitly accounted for in the model scheme. The relative number concentration of these particles compared to inorganics and oxygenated organic compounds of limited hygroscopicity plays an important role in determining the CCN number. Furthermore, expanding the different composition/mixing state schemes to predictions of cloud droplet number concentration in a cloud parcel model highlights the dependence of cloud optical properties on the state of mixing and hygroscopic properties of the different aerosol modes, but shows that the relative differences between the different schemes are reduced compared to those from the CCN model.

1 Introduction

The indirect influence of aerosol particles on the radiative balance of the atmosphere through changes in cloud droplet (N_d) number and persistence of clouds, known as the "aerosol indirect effect" (Twomey, 1974; Albrecht, 1989), carries the largest uncertainty amongst the presently known causes of radiative forcing (IPCC, 2001; 2007).

ACPD

8, 5629–5681, 2008

McFiggans et al. (2005) review much of the recent investigative work aiming to better characterise the physical and chemical parameters determining the relationship between the aerosol size distribution and chemical composition and cloud condensation nuclei (CCN). Whilst much progress is reported on our understanding of activation processes, McFiggans et al. (2005) outline measurement requirements which would further this knowledge, principally details of the physical and chemical nature of Aitken and small-accumulation mode aerosol in tandem with measurements of the CCN activation spectrum.

Recent CCN studies reported in the literature have addressed the relative importance of the size distribution, particle composition and mixing state in determining CCN activation, but there is disagreement on the relative importance of these parameters (Roberts et al., 2002; Feingold, 2003; Ervens et al., 2005; Mircea et al., 2005; Dusek et al., 2006a; Anttila and Kerminen, 2007; Hudson, 2007; Quinn et al., 2007). CCN closure studies are a useful approach to test our knowledge of the controlling physical and chemical properties and help verify experimental results. Several closure studies are reported in the literature where CCN activation measurements are compared with the output from equilibrium models which use Köhler theory to predict the CCN number concentration, N_{CCN}, from measured aerosol properties such as size distribution and composition or hygroscopicity. In the background atmosphere, several studies have been able to show closure between the measured and modelled results (Chuang et al., 2000; Dusek et al., 2003; VanReken et al., 2003; Rissler et al., 2004; Gasparini et al., 2006; Stroud et al., 2007). However, the particle distribution is more complex in locations such as urban areas where an air mass may comprise several different externally-mixed components, each exhibiting different chemical and physical characteristics (Lee et al., 2003; Alfarra et al., 2004; Zhang et al., 2004; Salcedo et al., 2006). Some components are shown to exhibit reduced activation properties with respect to inorganic salts, such as biomass burning plumes (Mircea et al., 2005; Lee et al., 2006; Clarke et al., 2007), humic-like substances (Dinar et al., 2006), secondary organics formed from oxidation of common biogenic emissions such as monoterpenes (Van-

CC BY

Reken et al., 2005; Varutbangkul et al., 2006) and black carbon (Dusek et al., 2006b; Kuwata et al., 2007). Other organic components are shown to activate more easily than their solubility might suggest (Raymond and Pandis, 2002; Hartz et al., 2006), but still much less than inorganic species. Particles that are generally hydrophobic or only slightly hygroscopic in nature are observed to significantly impact CCN properties of the atmosphere (Roberts et al., 2003; Roberts et al., 2006), and for internally mixed particles it appears that the moles of insoluble material is the most important chemical parameter affecting aerosol water affinity in the sub- (McFiggans et al., 2005) and super-saturated (Rissler et al., 2004; Ervens et al., 2007) regimes. In an urban area, where many such components may be externally- or internally-mixed with hygroscopic inorganic aerosol, modelling the CCN activation from basic physical properties is more difficult. Further information about the nature of the particles, such as size-resolved chemical composition or detailed properties of the organic component, may be required in order to successfully predict the CCN activation (Broekhuizen et al., 2006; Mochida et al., 2006; Quinn et al., 2007). Furthermore, recent work using data collected from areas under the influence of recent anthropogenic emissions has concluded that mixing state needs to be considered in order to resolve bias in the model predictions of N_{CCN}. Medina et al. (2007) conclude that an assumption of internal mixing in a CCN model considering size-resolved composition is responsible for a ~36% over-prediction of N_{CCN} as compared to measurements of polluted continental or semi-urban air masses in New Hampshire. Sensitivity studies on data collected at the Duke Forest site in North Carolina, showed that model predictions were highly sensitive to the assumed mixing state of the aerosol size distribution modes used for size distribution input, but lack of mixing state measurements precluded a quantitative evaluation of the effect of this parameter on closure (Stroud et al., 2007). Parameterisation of the mixing state of urban aerosol modes and their hygroscopic parameters has also been recently shown as important with respect to interpreting satellite retrieval data on urban aerosols (Wang and Martin, 2007).

Whilst aerosol-CCN closure studies improve our understanding of the importance of

physical and chemical properties for aerosol activation, they only refer to equilibrium conditions at one (or several) constant supersaturations, and thus neglect feedbacks on supersaturation and drop growth due to dynamic processes in clouds, which often dampen the effects of variations in CCN number. In a recent cloud model study, it was shown that composition only has a significant effect on cloud drop number concentration for an internally mixed aerosol population when competition for water is strong, i.e. at low updrafts, and/or high particle concentrations (Ervens et al., 2005). However, the role of the mixing state of aerosol was neglected in that study. Recent work shows that the uncertainty in predicting cloud droplet number (N_d) can be related to the uncertainty in N_{CCN} over a wide range of cloud microphysical conditions (Sotiropoulou et al., 2006). However, it has been shown that the relationship that is predicted between N_{CCN} and aerosol number concentration (N_a) often cannot be extrapolated to a relationship between N_{CCN} and N_d because the drop number concentration is influenced by updraft velocity (w) and shape of the aerosol size distribution (Warner, 1969; Twomey, 1977). In order to evaluate the effect of aerosols on cloud microphysics and optical properties, the shape of the cloud droplet distribution should be considered. Twomey's definition of the first indirect effect predicts a relationship between a change in the cloud droplet radius and cloud albedo with a change in aerosol number concentration for a constant liquid water content (Twomey, 1991). In the more general case, changes in water content should also be considered. It has been shown that when droplet distribution broadening is associated with an increase in drop concentration, the predicted Twomey effect is reduced (Liu and Daum, 2002). Conversely, when broadening accompanies decreases in drop concentration (e.g., via collision-coalescence), the Twomey effect is enhanced (Feingold et al., 1997).

The study of aerosol-CCN and aerosol-cloud-droplet closure and relationships inside and in the near-field outflow of large urban areas is of interest for two main reasons: (a) as the locus of intense primary particle emissions for a variety of sources which are often gradually internally mixed during the day due to coagulation and condensation of secondary species (from intense local emissions of secondary precursors), urban ar-

eas present one of the most challenging cases to test our understanding of the parameters controlling droplet activation and growth. Furthermore, recent work has shown that the principal uncertainty in predicting the magnitude of the global aerosol indirect effect arises from regions where the atmosphere is under the influence of urban emissions (Sotiropoulou et al., 2007); (b) at present more than 50% of the world population lives in urban areas and this fraction is growing, including numerous megacities, and thus the fraction of the polluted regions affected by urban aerosols (with atmospheric aging times $\leq$1 d) is non-negligible and growing rapidly (Molina et al., 2007).

In this study, we present results from the Study of Organic Aerosols at Riverside (SOAR-1) campaign held in Riverside, California, during July and August of 2005, a polluted area within the Los Angeles megacity. Riverside experiences both fresh emissions and the advection of urban aerosols with atmospheric ages of ~1–2 d, and thus is a good location to study the aerosol properties encountered inside and in the near-field outflow of megacities. We investigate the diurnal cycles of urban aerosol and CCN and use an activation model to probe the influences of size distribution, chemical composition, and mixing state on CCN. We use a CCN model employing increasingly complex cases of composition and mixing state, which highlight the importance of the mixing state of the various aerosol species. In addition to CCN predictions, we use these approaches as input data for a cloud model that we initialize with the measured size distributions and the different cases of composition and mixing state that are used to predict CCN number concentrations. We use the cloud model results to evaluate the extent to which the impact on CCN arising from differences in aerosol composition and mixing state typical of an urban area can affect cloud droplet concentrations and cloud optical properties.

2 Experimental description

The city of Riverside lies about 80 km east of the Pacific coast on the eastern edge of the Los Angeles (LA) – San Bernardino – Riverside conurbation, population 18 million.

CC BY

The prevailing westerly winds advect the accumulated pollution from the densely populated coastal and downtown LA areas and upwind farmlands eastwards towards Riverside. During this process, the pollution is largely confined to the LA basin by inversions which cap the highly polluted boundary layer air within the surrounding topography. The SOAR-1 campaign, conducted between 16 July and 15 August 2005, sampled at a location on the University of California at Riverside campus, about 1 km east of Highway 60 carrying commuting traffic to the LA area. The meteorological conditions during the summer campaign were very consistent, with a clear diurnal cycle, low cloud cover and temperatures generally peaking around 35 to 40°C in the afternoon and reaching a low of 15 to 20°C in the early morning. The location and weather conditions combine to produce a very polluted atmosphere consisting of a complex mixture of locally-emitted traffic emissions combined with high advected levels of primary and secondary aerosols.

The aerosol inlet was approximately 7 m above ground level. A bypass flow was used to facilitate the use of a 2.5 μm cut-off cyclone designed for a 10 lpm flow rate (URG-2000-30EN, www.urgcorp.com/cyclones) on the inlet and minimize losses in the line. The inlet flow was dried using either Nafion driers (PermaPure PD Series, www.permapure.com) or silica gel diffusion dryers before passing through Y stainless steel flow splitters (Brechtel Manufacturing, Inc., www.brechtel.com) for analysis by the various instruments. The aerosol size distribution was measured from 3 nm to 32 μm using a combination of two Scanning Mobility Particle Sizer systems (SMPS, TSI Model 3080, www.tsi.com) and an Optical Particle Counter (OPC, Grimm Model 1.110, www.grimm-aerosol.com). A time series of particle effective density was available for the latter stage of the campaign from the combination of an SMPS system with the Aerosol Particle Mass Analyser (APM, Kanomax, www.kanomax-usa.com) (McMurry et al., 2002). Elemental carbon (EC) and organic carbon (OC) mass measurements were available from the commercially available Sunset Labs Semi-Continuous EC/OC Analyzer (www.sunlab.com).

Size-resolved chemical composition information was available from an Aerodyne

CC BY

Time-of-Flight Aerosol Mass Spectrometer (ToF-AMS) (Drewnick et al., 2005; DeCarlo et al., 2006). The AMS uses an aerodynamic lens to focus particles into a particle time-of-flight chamber to separate aerosol according to their vacuum aerodynamic diameter and flash vaporize them under high vacuum, ionize the vapors by electron impact, and analyze the ions with a time-of-flight mass spectrometer. The mass spectrum is used to determine the mass loadings of several chemical species or groups of species (Allan et al., 2004), size segregated in the range of approximately 35 nm to 1 μm. In addition, size-resolved single-particle chemical composition was also acquired with a Aerosol Time-Of-Flight Mass-Spectrometer (ATOFMS) (Noble and Prather, 1996). This version of the ATOFMS uses a similar aerodynamic lens inlet as the AMS, but employs dual timing lasers to determine the arrival of single particles into a the focus point of a Nd-YAG laser which desorbs and ionizations particle constituents into both positive and negative ions, which are analyzed by dual time-of-flight mass spectrometers. Both instruments measure the size-resolved chemical composition according to vacuum aerodynamic diameter, d_{va}, defined in DeCarlo et al. (2004). A comparison and discussion of the ATOFMS, AMS, and two other laser ablation instruments is given by Middlebrook et al. (2003). The combination of the two provides an extensive data set including both quantitative size-resolved chemical information and a direct determination of the mixing state of the aerosol from single particle analysis.

The CCN activation properties of the aerosol ensemble were measured at various different supersaturations using the Continuous Flow Streamwise Thermal Gradient CCN Chamber (Droplet Measurement Technologies, Boulder, CO, available at: www.dropletmeasurement.com) (Roberts and Nenes, 2005; Lance et al., 2006). This new CCN instrument has greatly facilitated CCN research by providing a rapid, precise, and stable continuous flow instrument that is commercially available and that can be interfaced to other continuous flow instruments. During the SOAR campaign the instrument was set up to record CCN activation at supersaturation set points of S=0.1, 0.3, 0.5, 0.7 and 0.9% at 30-min intervals. The actual operational supersaturation in the instrument was calculated from the instrument temperature and flow readings using

CC BY

the model of Lance et al. (2006), and used in custom software to analyze the flow rate, temperature and pressure variations within the instrument and thus eliminate errant readings such as those during unstable or rapidly changing conditions.

3 Methods

To investigate the relative importance of the physical and chemical characteristics and the mixing state of the aerosol on their CCN activation properties, the CCN model described by Ervens et al. (2007) was used to predict the CCN activation for comparison to the measurements from the CCN chamber using a number of different composition and mixing state schemes. The model considers particles consisting of an internal mixture of very hygroscopic material, with the properties of ammonium sulphate, with a less-hygroscopic organic component. A further completely non-activating component, which is externally mixed with respect to the organic and ammonium sulphate particles, can also be introduced into the model cases. The CCN activation is calculated at the modeled supersaturation in the CCN chamber rather than the nominal set point values.

The hygroscopicity and CCN activity of the individual model components can be summarized by considering a single parameter, κ (Petters and Kreidenweis, 2007):

$$\kappa = M_w/\rho_w \Sigma(\nu\Phi_i/M_{si}\rho_{si}) \quad (1)$$

where ν is the number of molecules or ions a salt in solution dissociates into (Van't Hoff factor), Φ is the osmotic coefficient, M_w and M_s are the molecular weight of water and the solute, and ρ_w and ρ_s are the density of water and the solute respectively. Using this representation, it is shown that the relationship between the critical supersaturation and diameter can be defined using the κ parameter, with highly soluble materials exhibiting κ values around unity. Moderately hygroscopic organic species such as levoglucosan and malonic acid are shown to have κ values in the range 0.01 to 0.5, whilst hydrophobic particles would exhibit κ values approaching zero (Petters and Kreidenweis, 2007). Hygroscopicity or CCN measurements of various secondary

CC BY

organic aerosol (SOA) compounds formed atmospheric simulation chambers give derived κ values of around 0.06 to 0.2 (VanReken et al., 2005; Varutbangkul et al., 2006; Prenni et al., 2007), whereas oxidized primary organics have κ values of around 0.01 or less (Petters et al., 2006). We thus use κ values for our base case model of ~0.5 (ammonium sulphate) for the inorganic fraction and ~0.01 for the organic fraction. The sensitivity of the model to increasing the hygroscopicity of the organics is later studied. Although it was observed during the SOAR campaign that the nitrate mass concentrations were broadly similar to the sulphate, use of the model components described above is consistent with earlier work (Koehler et al., 2006; Ervens et al., 2007), and unlikely to introduce much error as ammonium nitrate is also a soluble compound with a propensity to readily form CCN . It has a κ value of 0.78, similar to ammonium sulphate (Petters and Kreidenweis, 2007), thus the activation diameters do not vary greatly (47 nm as compared to 42 nm for S=0.5%). Hence the two compounds are interchangeable in this model scheme, to good accuracy.

In all model variants, the SMPS size distribution and AMS chemical composition measurements provided the basis for the model calculations. Several different composition modes were determined using the mass spectrometers for input to the CCN model. In the urban atmosphere, small mode organic (SMO) particles are often observed with the AMS, which many studies have shown are typically externally-mixed with respect to a more aged, larger diameter internally-mixed mode of organics and inorganics (Lee et al., 2002; Alfarra et al., 2004; Zhang et al., 2004; Bein et al., 2005; Tolocka et al., 2005; Murphy et al., 2006; Niemi et al., 2006; Salcedo et al., 2006; Molina et al., 2007; Zhang et al., 2007). If the larger-diameter accumulation mode is assumed to maintain a consistent composition across its size range (due to its longer "integration time" for atmospheric aging), then the organic/inorganic ratio for this entire mode can be estimated as the measured ratio at the larger diameters where there is no influence from smaller, externally mixed modes in the size distribution. The SMO mass concentration can then be calculated by subtracting the estimated accumulation-mode organic size distribution estimated in this manner from the total measured organics, as

CC BY

demonstrated in Fig. 1. As expected, the SMO mass is significant at small diameters and falls to zero at d_{va}~300–400 nm. These mass loadings are converted to mobility space for direct comparison to the SMPS and input to the model using measured values of the particle effective density, using diurnal cycle measurements taken using the DMA-ATOFMS technique (Spencer et al., 2007) and from APM measurements in the work of Geller et al. (2006). The effective density of dry particles can also be estimated from the particle composition using estimated values for the different particle components. It is noted that these different techniques for calculating the particle effective densities have different dependencies on the particle morphology (DeCarlo et al., 2004), although they return similar results, with values around 1.2 to 1.4 g cm^{-3} for accumulation mode particles.

The SMO mass in urban areas can be further resolved into several components using factor analysis of the AMS mass spectra. Components such as hydrocarbon-like organic (HOA) and several types of oxygenated organic aerosol (OOA) (Zhang et al., 2005a; Ulbrich, 2006; Lanz et al., 2007; Ulbrich et al., 2008) are extracted, and they allow the introduction of further complexity into the compositional data in the model. The HOA fraction is assumed to represent fresh, carbonaceous traffic and other combustion emissions and was shown by Quinn et al. (2007) to be an important parameter influencing CCN activation in urban plumes measured over Houston, Texas. On the other hand, OOA is thought to be representative of local or regional SOA (Zhang et al., 2005c; Ulbrich, 2006; Lanz et al., 2007; Zhang et al., 2007). Similar to the observations of Zhang et al. (2005b) in Pittsburgh, a diurnal cycle was observed in the HOA and OOA fractions during the SOAR campaign[1]. The fraction of the SMO mass resolved as HOA was highest in the morning when the site was under the greatest

[1]Docherty, K. S., Stone, E. A., Ulbrich, I. M., DeCarlo, P. F., Snyder, D. C., Schauer, J. J., Peltier, R. E., Weber, R. J., Murphy, S. M., Seinfeld, J. H., Grover, B. D., Eatough, D. J., and Jimenez, J. I.: Apportionment of Primary and Secondary Organic Aerosol in Southern California during the 2005 Study of Organic Aerosol in Riverside (SOAR), submitted to Environ. Sci. Technol., 2008.

CC BY

influence from fresh traffic emissions. The OOA fraction dominated in the afternoon as photochemically-aged air was advected to the site from the Los Angeles basin. Biomass burning made a negligible contribution to particle concentrations during the SOAR-1 period, based on low satellite fire counts, and chemiscal markers from the AMS, ATOFMA, and GC-MS analysis[1].

There are two important classes of atmospheric aerosol that are not measured using the AMS. First, dust particles, which are often observed over Riverside with its location west of a large desert region. However, during the SOAR-1 study the winds were not favourable for the advection of dust to the sampling site and this aerosol component was not a significant feature of the aerosol distribution (Spencer et al., 2007). Second, elemental carbon (EC) particles are also not measured using the AMS (although non-refractory components internally mixed with them are (Slowik et al., 2004)), thus the methodology of Zhang et al. (2005b) was employed to infer the size distribution of black carbon by scaling the measurements of total EC mass to the observed HOA size distribution. A relationship is first derived between the observed HOA and EC mass; a regression line is calculated and then used to scale the HOA distribution to produce an estimated EC mass size distribution. In this case the HOA size distribution was calculated following the methodology of Zhang et al. (2005c), by subtracting 2% of the integrated signal at m/z 44 from the integrated signal at m/z 57 (to account for interferences from OOA in the mass spectra) and normalizing to the bulk HOA measurement. Figure 2 shows the resulting size distributions of the weekday average from 06:00–07:00 h of the particle mass fraction, HOA and estimated EC. The EC distribution is very similar to that of the HOA, but similarly represents only a small fraction of the organic mass.

The diurnal cycle for the measured CCN activated fractions at various supersaturations, the HOA and SMO mass fractions of total organics, and the average size distributions from the SMPS are shown in Fig. 3. There is a clear diurnal variability in both the size distribution, which shifts to larger diameters during the afternoon, and the composition, which shows the largest HOA fraction in the morning rush-hour. Both

CC BY

exhibit trends which correlate with the diurnal changes in the CCN activation, indicating that both influence the CCN activation properties at Riverside, but the variation in the total SMO fraction (which includes both HOA and OOA mass) over the diurnal cycle is small. Given the observed repeatable diurnal cycle and the improved signal-to-noise obtained by averaging, the measurements were averaged to a diurnal cycle over the weekday period for input into the model in 24 h-long steps. Large changes in emission scenarios of urban areas, and the subsequent impact of urban emissions on the local atmospheric aerosol distribution, may occur between weekends and weekdays, and also between Saturday and Sunday (Harley et al., 2005). Such differences have been shown to exist in the Los Angeles basin (Lough et al., 2006) and given the much reduced statistics, weekends were excluded from the analysis. Averaging to a diurnal cycle is useful to improve counting statistics in the size-resolved composition data as the noise in individual measurement cycles can often introduce unacceptable error into the model predictions. In addition, given the aim of this work to compare various model schemes rather than attempt perfect closure, any small errors induced through diurnal averaging are not critical to the overall conclusions. The various model schemes presented in this paper are described below and outlined in Table 1. Figure 4 illustrates the size-resolved compositions used in the models.

Case 1. Complete internal mixture

Following the methodology of Ervens et al. (2007), in this case the submicron aerosol ensemble is considered as perfectly internally mixed, that is, the aerosol maintains the same (average) chemical composition across the entire particle size range. The inorganic (organic) fraction of the aerosol is calculated using the bulk inorganic (organic) fraction measured by the AMS.

Case 2. Complete external mixture

Using the size-resolved inorganic fraction measured by the AMS, the organic and inorganic components in the model are considered to be externally mixed at all diameters; the organic fraction is treated as entirely non-activating. Whilst this is clearly an atmospherically-unrealistic case, it is useful to demonstrate the opposite extreme of mixing state from case 1 and the effect it has on the model predictions. It is also relevant to global models, since these typically represent the different aerosol components as externally mixed (Textor et al., 2006).

Case 3. Using size-resolved composition with internal mixture at each size

The aerosol ensemble maintains the same composition at each particle size class, but the inorganic fraction, and thus the κ value, can vary across the size range to account for the dominance of the organic component at the smaller particle diameters. The inorganic fraction at each size is the measured size-resolved inorganic fraction from the AMS. To account for the mass not measured by the AMS, the estimated EC size distribution is considered externally-mixed and non-activating at all diameters.

Case 4. External mixture of small diameter organics

As for case 3, except that, in addition to the estimated EC, the SMO are considered to be externally-mixed with respect to the background population and treated as non-activating in the model. This small mode has been observed to be externally-mixed from the large diameter mixed mode and largely hydrophobic in a number of hygroscopicity studies (Svenningsson et al., 1992; McMurry et al., 1996; Weingartner et al., 1997; Swietlicki et al., 1999; Cubison et al., 2006).

CC BY

Case 5. External mixture eliminating hydrocarbon-dominated small diameter organics

As for case 4, except that the organics are treated as two different populations. One part, proxied by OOA in the AMS, is treated as weakly-hygroscopic organics in the model with a κ value=0.01, internally-mixed with the inorganic fraction. The remaining fraction is considered totally non-activating in the model, as determined by measurements of the HOA from the AMS, and single particle information from the ATOFMS.

4 Results

Figure 5 shows the scatter plots between the predicted and measured CCN activated number for the five different supersaturation set points for case 1 (C1, complete internal mixing). The particle size distribution is considered as an internal mixture of two species of differing hygroscopicity; no entirely non-activating number fraction (e.g. EC) is considered. In all cases the model prediction is only weakly correlated with the measurements (R^2~0.3), which indicates that, while the diurnal variations in the number concentration and size distribution exhibited in Fig. 3 do influence the CCN activation, these properties alone cannot explain all the variation in the CCN measurements. The model also over-predicts the CCN number concentration by a factor of about three at S=0.3 to 0.9%. The much larger over-prediction at the lowest S=0.1% was also observed by Ervens et al. (2007) and attributed to problems with either temperatures (Roberts, G., personal communication) or high flow rates (Lance et al., 2006) in the CCN instrument, which may not allow for enough time for particles to reach sizes large enough to be counted by the OPC at the exit of the CCN chamber. The results are thus shown for S=0.1% for all the model schemes, but disregarded in the discussion. The over-prediction at $S \geq 0.3\%$ is expected as many particles smaller than 200 nm are really organic-dominated and thus, even if consisting of water-soluble organic compounds (WSOC), are expected to be only weakly-hygroscopic in nature (Clarke et al., 2007). However, in the model they are assumed to maintain a sizeable, very hygro-

ACPD
8, 5629–5681, 2008

scopic, inorganic component. It has been previously shown how a small amount of hygroscopic material on a hydrophobic particle can greatly influence its CCN activation properties (Bilde and Svenningsson, 2004), and thus the assumption that there is inorganic material in all the particles over the entire diameter range falsely increases the CCN concentration in the model.

The most extreme opposite case from C1 is the entirely externally-mixed case C2 as shown in Fig. 6; it is clear that the modeled CCN number concentrations are drastically reduced from C1, and C2 tends to under-predict the measurements at the larger supersaturations. The correlation between measurements and model is reduced with respect to M1 (R^2~0.2), which indicates that the predictive skill of the model is reduced along with the bias. Whilst this demonstrates the large influence of assumed mixing state on CCN prediction in an urban area, the model results cannot be considered valid given that the assumption of complete external mixing is not atmospherically feasible. It is likely that any agreement or correlation with the measurements results from the specific combination of size distributions and mass loadings observed at Riverside. At other locations, model predictions using a similar mixing state assumption have also not been able to reach agreement with measured CCN numbers (Broekhuizen et al., 2006). We therefore introduce three model schemes of increasing complexity using detailed compositional data from the AMS and ATOFMS.

Figure 7 shows the scatter plots between the model and measurements for the CCN model using internally-mixed, size-resolved composition (Case 3, C3). In order to account for size-resolved mass not measured by the AMS, the estimated EC distribution is considered to be externally-mixed and entirely non-activating in this model.

In the size-resolved case, the smallest particles are almost exclusively organic in nature, as shown in Fig. 4, whereas the larger particles still maintain a large hygroscopic inorganic component. However, unlike the results of Broekhuizen et al. (2006), in which the use of size-resolved composition from an AMS in a CCN model with a hydrophobic organic fraction was shown to achieve closure on an urban dataset, in this work the model still over-predicts the CCN concentration by around a factor of 2 at the four

CC BY

larger S. However, the correlation between the measurements and the model improves from M1, with R^2 values ~0.4, indicating that the variation in size distribution alone is not capturing all the dynamics of the diurnal cycle in the CCN, and that including the size-resolved composition incorporates additional information that improves the predictions. Although the estimated EC is treated as non-activating, it is likely that many of the small diameter organics measured by the AMS are fresh traffic emissions and thus also carbonaceous and truly non-activating in nature. However, in this model they are treated as slightly hygroscopic with a κ value of 0.01, similar to oxidized POA and SOA (Petters and Kreidenweis, 2007). Importantly, the assumption of even small quantities of inorganic mass on the small diameter particles falsely increases the number of CCN, which leads to the observed over-prediction. It thus becomes necessary to use a more complex treatment of the mixing state of the SMO particles.

Figure 8 shows the scatter plots between the CCN model and measurements where all the SMO particles and estimated EC are treated as externally-mixed and entirely non-activating (Case 4, C4). It was shown in Fig. 3 that the diurnal variation in the SMO was small and indeed, the skill of the model is reduced with the addition of this externally-mixed component which does not follow a clear diurnal pattern similar to the CCN. However, the agreement is improved significantly with respect to C3 with over-predictions ranging from zero to 49%.

Earlier work has shown that it is appropriate to treat slightly-hygroscopic organic material as hydrophobic in CCN model studies (Abbatt et al., 2005; Broekhuizen et al., 2006; Ervens et al., 2007; Prenni et al., 2007). Although the SMO mode estimated here is likely to contain both HOA and OOA fractions, the latter of which are likely to be slightly hygroscopic, it appears as though, for the CCN model, treating the small-mode slightly hygroscopic WSOC material as hydrophobic and thus CCN inactive is also justified in this location.

Recent work has suggested that the HOA fraction of urban aerosol has a significant influence on CCN activation (Quinn et al., 2007). In Fig. 3, the diurnal cycle of the HOA mass fraction was shown to broadly anti-correlate with the CCN activation. Thus, a

CC BY

case is developed where only those organics deemed hydrocarbon-like in nature in the AMS are considered non-activating in the model; the remainder are left to be treated as a component with a κ value of 0.01 in keeping with the previous model cases (Case 5, C5). The quantification of the HOA in C5 and the assumption that it has a source in local emissions and is carbonaceous in nature are supported by single particle information from the ATOFMS. When analyzing those particle mass with d_{va}<130 nm, where the AMS indicates virtually all the particles observed are in the small organic mode, several different externally-mixed particles types are observed (Spencer et al., 2007) with the ATOFMS. The mixing ratio of the different particle classes is found to follow a clear diurnal cycle during the weekday period, with the fraction of those organic particles that are exclusively carbonaceous with no hygroscopic material, classed here as "fresh", reaching a maximum at 06:00 h of around 0.35. The fraction of these particles is observed to decrease to around 0.15 at noon and remain constant through the afternoon. All the remaining particle classes, collectively grouped under the "partially aged" term here, contain oxygenated organic compounds and amines. The fraction of particles with d_{va}<130 nm classed as hydrocarbon-like in the AMS, and thus treated as non-activating in the model scheme of Fig. 9, match the number fractions from the ATOFMS very closely, varying between 0.15 and 0.35 on the same diurnal cycle. As these carbonaceous particles are likely to be extremely inactive with respect to CCN activation (Dusek et al., 2006b; Ervens et al., 2007), their treatment as totally non-activating in a simple model appears justified.

Figure 9 shows the scatter plot between the model and the measurements for C5, where the model over-predicts by between 68 and 100%. This is a greater over-prediction than observed for C4, suggesting that developing a parameterization for the mixing state and hygroscopicity of not only the HOA fraction, but also the SMO, is important for modeling CCN activation in this location. However, as a result of integrating a non-activating component with a diurnal cycle broadly anticorrelated with that of the CCN fraction, the skill of the model is improved from C4, with R^2 values around 0.4. Nonetheless, the over-prediction in C5 suggests that the oxygenated organics

CC BY

observed in the AMS and ATOFMS for the SMO are also largely CCN inactive in this dataset. Figure 10 shows the weekday diurnal cycles in both the aerosol number from the condensation nucleus (CN) counter and activated CCN at S=0.5%, together with the diurnal cycles in CCN at S=0.5% predicted by the five different models. The variation in the size distribution allows C1, with limited compositional influence, to capture the general diurnal profile of the activated CCN. By declaring as non-activating a component broadly anti-correlated with CCN activation, C5 most accurately captures the diurnal cycle in the CCN, while C2 and C4 are closest to reaching agreement with the measurements. However, all of the models over-predict most strongly during the CN peak in the morning rush-hour period, where only a subset of the emissions particles are activated (this is clearly shown by the activated fraction traces in Fig. 3). Further suppression of the CCN activation properties of the fresh traffic emissions particles that dominate the number concentration during this period would be required in the model in order to reach agreement with the measurements. It is possible that small, fractal, emissions particles which are classified by the mobility analysis as larger than their true size (DeCarlo et al., 2004) are then activated in the CCN model. In addition, recent work has shown that kinetic limitations on cloud droplet formation, which are not considered in this study, may significantly slow the activation of particles in polluted urban areas (Ruehl et al., 2007). The temporal pattern of CCN number concentration observed at Riverside, with the largest deviation from the modeled values observed during the peak of fresh urban emissions, can be at least qualitatively explained through this effect.

5 Discussion

Although Fig. 8 shows a good degree of closure between the model and the measurements when the SMO and EC particles are treated as non-activating, the model is dependent on the basic properties of the weakly-hygroscopic OOA which is internally mixed with the inorganics in the large mixed mode. Changing the κ value of the weakly-

hygroscopic OOA from 0.01 (cf. oxidized POA (Petters et al., 2006), Fig. 8) to 0.13 (cf. chamber studies of SOA (Asa-Awuku et al., 2007)) for the organic fraction increases the slope of the regression lines by between 14 and 30% over the different supersaturation values, as shown for S=0.5% in Fig. 11. Further increasing the large-mode organic κ value to that of Ammonium Sulphate decreases the skill of the model and further increases the degree of over-prediction in the model. It is noted that decreasing the κ of the organics to values approaching zero does not significantly decrease the degree of over-prediction at S=0.5% in the model.

Unlike in our study, Broekhuizen et al. (2006) achieved CCN closure on an urban dataset using a model case similar to C3, but treating the organics as hydrophobic in nature. However, Fig. 12 shows that at Riverside, the size resolved model case C3 is largely insensitive to the organic hygroscopicity, where applying a κ value as low as ~0.0004 does not greatly decrease the level of over-prediction observed in the model. In this methodology it is clear that the incorrect assumption of internal mixing causes small quantities of inorganic mass on the smaller particles to dominate the CCN activation properties.

In summary, although it is clear the model is somewhat sensitive to the assumptions used about the inherent properties of the weakly-hygroscopic organics in the large mixed mode, it is clear that well-correlated closure can only be achieved using additional treatment of the mixing state beyond the use of a size-resolved organic fraction. The large diameter mixed mode is ubiquitously observed throughout the northern hemisphere and many field studies demonstrating this are summarized in Canagaratna et al. (2007). The organic component of this mode was shown by Ervens et al. (2007) to be largely hydrophobic with respect to CCN activation at a marine background location. Given that the best agreement is reached for C4 when the organic κ value is small, this finding is also supported here in an urban location, highlighting common activation properties of the ubiquitous large mode over different geographical settings.

Given that some previous studies have been able to show closure without explicit treatment of externally-mixed modes, we consider to what extent it is necessary to

CC BY

consider externally-mixed SMO aerosol in CCN modeling over the global atmosphere. It is clear that the background location studies would not need treatment of a fresh emissions component that is absent in such locations. Indeed, C1, using the assumption of internal mixing, was successfully used to achieve closure on the measurements from the background marine site at Chebogue Point, Nova Scotia (Ervens et al., 2007), but in that case the aged (≥2 d) pollution and remote continental aerosol did appear internally-mixed and soluble in nature and thus the inorganic material was indeed observed to be spread across the whole particle diameter range, indicating that the internal mixing assumption is appropriate for this type of aged air mass. Many air masses worldwide are likely to exhibit characteristics somewhere between the two opposite cases observed at Chebogue Point and Riverside. It has been shown that urban emissions are transformed by atmospheric processes such as coagulation and condensation as they are diluted during advection downwind from the emissions area (Riemer et al., 2004; Cubison et al., 2006; de Gouw et al., 2006; Volkamer et al., 2006; Zhang et al., 2007). The timescales for the primary hydrophobic mass of these aerosols to be no longer a significant component of the particle mass (mainly due to dilution with regional air and condensation of secondary species) were found to be between 1 to 2 d. After this time period, the less-hygroscopic mode is no longer visible in hygroscopicity measurements (Cubison et al., 2006) and it is thus unlikely that explicit treatment of the non-activating number fraction would be required beyond this timescale to achieve CCN closure. It is clear that, with the expansion of urban population and megacities worldwide, that there are significant areas of the atmosphere, both over these metropolitan areas and immediately downwind, where such calculations could benefit from inclusion of a simple treatment of the non-activating particles such as that presented here.

6 Cloud droplet model

6.1 Model parameters

While the CCN calculations are performed for equilibrium conditions using the Köhler equation, i.e. for a prescribed supersaturation, in a cloud parcel model the supersaturation is determined by (i) a dynamic term that represents the source of supersaturation and (ii) the condensation term that depends on the size and composition of the particles, and the supply of water vapour. Assuming adiabatic conditions for an ascending air parcel until a maximum liquid water content (0.3 g m^{-3}) is reached, we compare the cloud properties that are predicted for model cases C2, C3, C4 and C5 to those predicted for the internally-mixed case C1. We somewhat arbitrarily define the total drop number concentration N_d as the population of all particles (drops) >2 μm in diameter, unlike in CCN studies where we consider the number of activated particles according to Köhler theory.

6.2 Predicted cloud droplet number concentrations N_d

In Fig. 13, we compare the CCN concentrations predicted for the internally-mixed cloud model case C1 to those predicted for C2, C3, C4 and C5, for S=0.5%. The slopes were observed to be mostly independent of the value of S and thus results are only shown for one supersaturation. The only difference in this trend is represented by C4, as a significant fraction of particles are externally-mixed from the large mode and thus the number of activated particles increases more in C1 than C4 with increasing supersaturation, as in C4 the critical diameter moves into the region where many SMO particles are considered non-activating.

Superimposed on the same plot are predictions of N_d that result from two different updraft velocities (w=50 cm s^{-1} and w=300 cm s^{-1}) It should be noted that the maximum supersaturations reached in the modelled air parcels differ from the single supersaturation value used in the comparisons detailed above (S_3~0.5%) as they

depend on w, aerosol composition and size distributions: At w=50 cm s^{-1}, the calculated maximum supersaturations are ~ 0.1–0.4% whereas those at the higher updraft (w=300 cm s^{-1}) are in the range of 0.4–1%. Both the comparisons for C3 and C5 vs. N_{CCN} (C1) exhibit very similar slopes. C3 and C5 only differ by the properties of the small particles (<~200 nm diameter) which are assumed to be an externally-mixed non-activating mode in M5 while they are hygroscopic and internally-mixed in case C3. Such small particles are mainly just above the typical critical activation diameter and, in the unlimited water supply in the Köhler CCN model, will activate. However, in the cloud model, under competition for water vapour, they may not grow to the 2 μm cut-point before the maximum liquid water content is reached.

In all cases N_d is much smaller than N_{CCN} for low updraft velocity because (i) less particles are activated and grow to drop sizes in an ascending cloud parcel due to limited growth time and limited supply of water vapour due to competition for available vapour and (ii) we apply different definitions for N_{CCN} (=particles that exceed their critical size according to Köhler theory) and N_d (particles that exceed the diameter of 2 μm), respectively.

In general, all regression lines for N_d in Fig. 13 show the same trend as predicted for N_{CCN} but have higher slopes. This reiterates the point that composition effects on CCN are not the same as composition effects on N_d (Ervens et al., 2005), and that differences are reduced when considering effects on N_d. However, the differences in the slope for w=50 cm s^{-1} and w=300 cm s^{-1} are different from the results of Ervens et al. (2005) where it was found that at higher updraft velocities composition effects are reduced (and, thus, should exhibit slopes closer to the 1:1 line), in our case the opposite is observed. However, the latter study considered only a pure internally mixed aerosol (cf. C1 in this study) and no change in soluble fraction and/or mixing state with size. In the current data set, smaller particles are less hygroscopic (or even completely non-activating) and with increasing updraft, for these cases, fewer particles can be activated compared to the more hygroscopic aerosol population assumed in C1.

CC BY

6.3 Dispersion of cloud droplet size distributions

At constant liquid water content (LWC), an increase in aerosol number leads to an increase in cloud drop number, and decrease in droplet size at constant LWC (Twomey, 1977). Twomey's theoretical calculations assume that the shape of the drop size distribution is constant. However, observations in polluted areas have shown that an increase in drop number concentration associated with an increase in anthropogenic emissions usually leads to an increase in the relative dispersion, D, defined as the ratio of the standard deviation to the mean radius, of the drop size distribution at the small-drop end (Liu and Daum, 2002). This effect results from the fact that condensation growth tends to narrow the size distribution. In polluted conditions, the increased competition for water vapour results in less growth per droplet, and therefore less spectral narrowing due to the condensation process.

In Fig. 14 we compare D of the resulting cloud droplet size distributions for the five different models at w=50 cm s^{-1}. We only show results for w=50 cm^{-1}, where the supersaturation is small and relative importance of the condensation (composition) term is higher (Ervens et al., 2005). Again, we compare the results of model cases C2 to C5 to those of the pure internal mixture (C1). Figure 14 shows similar D for C1, C3 and C5 even though C1 exhibits larger drop number concentrations, which is a function of the mixing state and composition assumptions applied in the different models. For the large particles, a small hygroscopic fraction is sufficient to initiate efficient growth and, thus, the largest drop diameters do not differ much for cases C1, C3 and C5. However, for smaller size particles, differences in hygroscopicity change the growth rates of individual particles, and, thus, the shape (breadth) of the resulting drop size distribution. This effect is even more pronounced since the most significant differences in hygroscopicity are in the size range of ~100 nm which is about the size of the smallest activated particles. Therefore the case where the SMO particles are considered externally-mixed and totally non-activating (C4) leads to a narrower size distribution because fewer drops are activated (many of the particles are not hygroscopic) and there is more condensation

ACPD
8, 5629–5681, 2008

growth per drop. The presence of a large number of externally mixed hydrophobic particles does not influence cloud properties and indeed this case resembles a somewhat clean case with smaller CCN and drop number concentrations.

6.4 Cloud susceptibility S

Cloud susceptibility S_{sc} is defined as the change in cloud albedo A for a change in drop number concentration N_d under conditions of constant cloud liquid water content, and fixed drop size distribution shape (Twomey, 1991):

$$S_{sc} = \left.\frac{\partial \ln A}{\partial \ln N_d}\right|_{\mathrm{LWP,shape}} = \frac{A(1-A)}{3N_d} \tag{2}$$

where albedo is calculated based on the expression by (Bohren, 1987) for a plane-parallel cloud:

$$A = \frac{(1-g)\tau}{2+(1-g)\tau} \tag{3}$$

with g= asymmetry factor (≈0.84) and τ= cloud optical depth. The liquid water path is ~80 g/m^2 for the cloud-top liquid water content of 0.3 g m^{-3} and the assumed cloud base temperature and pressure.

We have used the effects of aerosol on cloud albedo, as represented by Eq. (3) as a measure of the aerosol indirect effect and calculated S_{sc}, shown in Fig. 15 (for an updraft velocity of w=50 cm s^{-1}) for C1 to C5. At higher aerosol concentrations the response of cloud optical properties to the increase in aerosol number is smaller, i.e., the cloud susceptibility is lower. This is the case for C1, C3 and C5. In the external mixture of C4, the drop number concentration is lowest and thus C4 exhibits the highest values of S_s. The tendency to narrower size distributions in C4 decreases this effect to a small extent (Feingold et al., 1997), but the influence due to N_d is strongest.

This finding reinforces the importance of the mixing state of particles, as mediated by N_d, on cloud optical properties (e.g. Broekhuizen et al., 2006; Medina et al., 2007).

Small changes in the hygroscopicity of internally-mixed particles containing very hygroscopic material do not have a significant effect because of their small effect on N_d.

7 Conclusions

A number of different model schemes are presented for attempting CCN closure between measurements of the physical and chemical properties of urban aerosol at Riverside, CA, and their CCN activation. A CCN model is used to consider both internally- and externally-mixed aerosol populations, and it is shown that treatment of externally-mixed components is necessary to approach closure in a highly polluted urban area in the presence of freshly emitted particles. However, the over-prediction observed in all the models during the morning rush-hour indicates that there are additional effects influencing the CCN activation, such as further complexity in the mixing state, over-sizing of fractal particles by the SMPS, kinetic limitations to CCN activation, or possible bias in the measurements.

Size-resolved chemical composition is required to differentiate between the hygroscopic organic and inorganic aerosol components. In order to achieve good closure with significant correlation in this urban location using atmospherically-relevant assumptions for the internally-mixed hygroscopic organics in the model, and taking into account mass not measured by the AMS, it is necessary to treat non-activating urban emissions particles, here observed as EC and SMO, as externally-mixed with respect to the remainder of the aerosol population. In addition, it is found that the organic component of the accumulation mode exhibits CCN activation properties similar to those found in a coastal location (Ervens et al., 2007), behaving as effectively hydrophobic mass in the CCN model. Closure studies using the same model at further locations would help determine if the observed hydrophobicity of the SMO in Ervens et al. (2007) and this work is applicable for the hygroscopic large mixed mode which has been observed ubiquitously in northern hemisphere locations (Alfarra et al., 2004; Canagaratna et al., 2007).

ACPD
8, 5629–5681, 2008

In addition, we explored the extent to which such differences in composition translate into differences in predicted cloud microphysical and optical properties. The cloud model considers the role of supersaturation sources and sinks in an adiabatic air parcel that more closely reflects conditions in natural clouds than does the static supersaturation in a CCN counter where all the particles are given enough residence time to reach equilibrium conditions. As shown in previous model studies, in an adiabatically rising air parcel the maximum supersaturation is determined by both the updraft, and the size distribution/composition of the particles. The negative feedback between the vapour source and sink terms results in a reduced influence of composition on drop activation than for assumed equilibrium conditions, consistent with previous results of (Ervens et al., 2005). The size-resolved hygroscopicity of an internally mixed aerosol population influences both cloud drop number concentration and the shape of the cloud drop size distribution, and we have shown that these effects may enhance or counter one another in the calculation of the cloud susceptibility. However, significant decrease in the cloud drop number concentration as caused by a large fraction of externally-mixed non-activating particles overwhelms shape effects on cloud albedo and susceptibility. The only distinct composition differences occur if external vs. internal mixtures are compared, since the potential number of activated particles changes significantly. Thus, the mixing state of particles with sizes larger than critical diameters, and significant differences in the hygroscopic properties of separate modes have to be known in order to give a reliable estimate of aerosol influences on cloud microphysical and optical properties.

Acknowledgements. The authors would like to thank J. Ogren, B. Andrews and P. Sheridan of NOAA ESRL for the loan and instruction in use of the DMT CCN counter for the SOAR-1 campaign, T. Nenes of Georgia Tech. for use of the DMT CCN counter simulation model for calculation of the instrument operational supersaturation values, J. Schauer and D. Snyder for providing EC data, and P. Ziemann for hosting the field campain. G. Feingold and B. Ervens acknowledge support from NOAA's Climate Goal. This work was funded by US EPA STAR grants RD83216101-0 and R831080 and by NSF grant ATM-0449815. I. M. Ulbrich acknowledges a NASA Earth Science Fellowship (NNG05GQ50H). This paper has not been reviewed by either

funding agency and no official endorsement should be inferred.

References

Abbatt, J. P. D., Broekhuizen, K., and Kumal, P. P.: Cloud condensation nucleus activity of internally mixed ammonium sulfate/organic acid aerosol particles, Atmos. Environ., 39, 4767–4778, 2005.

Albrecht, B. A.: Aerosols, clouds and microphysics., Science, 245, 1227–1230, 1989.

Alfarra, M. R., Coe, H., Allan, J. D., Bower, K. N., Boudries, H., Canagaratna, M. R., Jimenez, J. L., Jayne, J. T., Garforth, A. A., Li, S.-M., and Worsnop, D. R.: Characterization of urban and rural organic particulate in the Lower Fraser Valley using two Aerodyne Aerosol Mass Spectrometers., Atmos. Environ., 38, 5745–5758, 2004.

Allan, J. D., Delia, A. E., Coe, H., Bower, K. N., Alfarra, M. R., Jimenez, J. L., Middlebrook, A. M., Jayne, J. T., and Worsnop, D. R.: A generalised method for the extraction of chemically resolved mass spectra from Aerodyne aerosol mass spectrometer data., J. Aerosol Sci., 35, 909–922, 2004.

Anttila, T. and Kerminen, V. M.: On the contribution of Aitken mode particles to cloud droplet populations at continental background areas – a parametric sensitivity study, Atmos. Chem. Phys., 7, 4625–4637, 2007, http://www.atmos-chem-phys.net/7/4625/2007/.

Asa-Awuku, A., Nenes, A., Gao, S., Flagan, R. C., and Seinfeld, J. H.: Alkene ozonolysis SOA: inferences of composition and droplet growth kinetics from Köhler theory analysis, Atmos. Chem. Phys. Discuss., 7, 8983–9011, 2007, http://www.atmos-chem-phys-discuss.net/7/8983/2007/.

Bein, K. J., Zhao, Y. J., Wexler, A. S., and Johnston, M. V.: Speciation of size-resolved individual ultrafine particles in Pittsburgh, Pennsylvania, J. Geophys. Res., 110, D07S05, doi:10.1029/2004JD004708, 2005.

Bilde, M. and Svenningsson, B.: CCN activation of slightly soluble organics: the importance of small amounts of inorganic salt and particle phase, Tellus B, 56, 128–134, 2004.

Bohren, C.: Mulitple light scattering of light and some of its observable consequences, Am. J. Phys., 55, 524–533, 1987.

Broekhuizen, K., Chang, R. Y. W., Leaitch, W. R., Li, S. M., and Abbatt, J. P. D.: Closure be-

tween measured and modeled cloud condensation nuclei (CCN) using size-resolved aerosol compositions in downtown Toronto, Atmos. Chem. Phys., 6, 2513–2524, 2006, http://www.atmos-chem-phys.net/6/2513/2006/.

Canagaratna, M. R., Jayne, J. T., Jimenez, J. L., Allan, J. D., Alfarra, M. R., Zhang, Q., Onasch, T. B., Drewnick, F., Coe, H., Middlebrook, A., Delia, A., Williams, L. R., Trimborn, A. M., Northway, M. J., DeCarlo, P. F., Kolb, C. E., Davidovits, P., and Worsnop, D. R.: Chemical and microphysical characterization of ambient aerosols with the Aerodyne aerosol mass spectrometer, Mass Spectrom. Rev., 26, 185–222, 2007.

Chuang, P. Y., Collins, D. R., Pawlowska, H., Snider, J. R., Jonsson, H. H., Brenguier, J. L., Flagan, R. C., and Seinfeld, J. H.: CCN measurements during ACE-2 and their relationship to cloud microphysical properties, Tellus B, 52, 843–867, 2000.

Clarke, A., McNaughton, C., Kasputin, V. N., Shinozuka, Y., Howell, S., Dibb, J., Zhou, J., Anderson, B., Brekhovskikh, V., Turner, H., and Pinkerton, M.: Biomass burning and pollution aerosol over North America: Organic components and their influence on spectral optical properties and humidification response, J. Geophys. Res., 112, D12S18, doi:10.1029/2006JD007777, 2007.

Cubison, M. J., Alfarra, M. R., Allan, J., Bower, K. N., Coe, H., McFiggans, G. B., Whitehead, J. D., Williams, P. I., Zhang, Q., Jimenez, J. L., Hopkins, J., and Lee, J.: The characterisation of pollution aerosol in a changing photochemical environment, Atmos. Chem. Phys., 6, 5573–5588, 2006, http://www.atmos-chem-phys.net/6/5573/2006/.

de Gouw, J. A., Warneke, C., Stohl, A., Wollny, A. G., Brock, C. A., Cooper, O. R., Holloway, J. S., Trainer, M., Fehsenfeld, F. C., Atlas, E. L., Donnelly, S. G., Stroud, V., and Lueb, A.: Volatile organic compounds composition of merged and aged forest fire plumes from Alaska and western Canada, J. Geophys. Res., 111, D10303, doi:10.1029/2005JD006175, 2006.

DeCarlo, P. F., Slowik, J. G., Worsnop, D. R., Davidovits, P., and Jimenez, J. L.: Particle morphology and density characterization by combined mobility and aerodynamic diameter measurements, Part 1: Theory, Aerosol Sci. Technol., 38, 1185–1205, 2004.

DeCarlo, P. F., Kimmel, J. R., Trimborn, A., Jayne, J. T., Aiken, A. C., Gonin, M., Fuhrer, K., Horvath, T., Docherty, K., Worsnop, D. R., and Jimenez, J. L.: A Field-Deployable High-Resolution Time-of-Flight Aerosol Mass Spectrometer., Anal. Chem., 78, 8281–8289, 2006.

Dinar, E., Taraniuk, I., Graber, E. R., Katsman, S., Moise, T., Anttila, T., Mentel, T. F., and Rudich, Y.: Cloud Condensation Nuclei properties of model and atmospheric HULIS, Atmos.

Chem. Phys., 6, 2465–2481, 2006, http://www.atmos-chem-phys.net/6/2465/2006/.
Drewnick, F., Hings, S. S., DeCarlo, P., Jayne, J. T., Gonin, M., Fuhrer, K., Weimer, S., Jimenez, J. L., Demerjian, K. L., Borrmann, S., and Worsnop, D. R.: A new time-of-flight aerosol mass spectrometer (TOF-AMS) – Instrument description and first field deployment, Aerosol Sci. Technol., 39, 637–658, 2005.
Dusek, U., Covert, D. S., Wiedensohler, A., Neususs, C., Weise, D., and Cantrell, W.: Cloud condensation nuclei spectra derived from size distributions and hygroscopic properties of the aerosol in coastal south-west Portugal during ACE-2, Tellus B, 55, 35–53, 2003.
Dusek, U., Frank, G. P., Hildebrandt, L., Curtius, J., Schneider, J., Walter, S., Chand, D., Drewnick, F., Hings, S., Jung, D., Borrmann, S., and Andreae, M. O.: Size matters more than chemistry for cloud-nucleating ability of aerosol particles, Science, 312, 1375–1378, 2006a.
Dusek, U., Reischl, G. P., and Hitzenberger, R.: CCN activation of pure and coated carbon black particles, Environ. Sci. Technol., 40, 1223–1230, 2006b.
Ervens, B., Feingold, G., and Kreidenweis, S.: Influence of water-soluble organic carbon on cloud drop number concentration., J. Geophys. Res., 110, D18211, doi:10.1029/2004JD005634, 2005.
Ervens, B., Cubison, M. J., Andrews, E., Feingold, G., Ogren, J. A., Jimenez, J. L., DeCarlo, P., and Nenes, A.: Prediction of CCN number concentration using Measurements of Aerosol Size Distributions and Composition and Light Scattering Enhancement Due to Humidity, J. Geophys. Res., 112, D10S32, doi:10.1029/2006JD007426, 2007.
Feingold, G., Boers, R., Stevens, B., and Cotton, W. R.: A modeling study of the effect of drizzle on cloud optical depth and susceptibility, J. Geophys. Res., 102(D12), 13 527–13 534, doi:10.1029/97JD00963, 1997.
Feingold, G.: Modeling of the first indirect effect: Analysis of measurement requirements, Geophys. Res. Lett., 30(19), 1997, doi:10.1029/2003GL017967, 2003.
Gasparini, R., Collins, D. R., Andrews, E., Sheridan, P. J., Ogren, J. A., and Hudson, J. G.: Coupling aerosol size distributions and size-resolved hygroscopicity to predict humidity-dependent optical properties and cloud condensation nuclei spectra., J. Geophys. Res., 111, D05S13, doi:10.1029/2005JD006092, 2006.
Geller, M., Biswas, S., and Sioutas, C.: Determination of particle effective density in urban environments with a differential mobility analyzer and aerosol particle mass analyzer, Aerosol

Sci. Technol., 40, 709–723, doi:10.1080/02786820600803925, 2006.
Harley, R. A., Marr, L. C., Lehner, J. K., and Giddings, S. N.: Changes in motor vehicle emissions on diurnal to decadal time scales and effects on atmospheric composition, Environ. Sci. Technol., 39, 5356–5362, 2005.
Hartz, K. E. H., Tischuk, J. E., Chan, M. N., Chan, C. K., Donahue, N. M., and Pandis, S. N.: Cloud condensation nuclei activation of limited solubility organic aerosol, Atmos. Environ., 40, 605–617, 2006.
Hudson, J.: Variability of the relationship between particle size and cloud-nucleating ability, Geophys. Res. Lett., 34, L08801, doi:10.1029/2006GL028850, 2007.
IPCC: Climate change 2001: Scientific basis, Third assessment of the Inter-governmental Panel on Climate Change, Cambridge Univ. Press, New York, 2001.
IPCC: Climate change 2007: Scientific basis, Fourth assessment of the Inter-governmental Panel on Climate Change, Cambridge Univ. Press, New York, 2007.
Koehler, K. A., Kreidenweis, S. M., DeMott, P. J., Prenni, A. J., Carrico, C. M., Ervens, B., and Feingold, G.: Water activity and activation diameters from hygroscopicity data – Part II: Application to organic species, Atmos. Chem. Phys., 6, 795–809, 2006, http://www.atmos-chem-phys.net/6/795/2006/.
Kuwata, M., Kondo, Y., Mochida, M., Takegawa, N., and Kawamura, K.: Dependence of CCN activity of less volatile particles on the amount of coating observed in Tokyo, J. Geophys. Res., 112, D11207, doi:10.1029/2006JD007758, 2007.
Lance, S., Medina, J., Smith, J. N., and Nenes, A.: Mapping the operation of the DMT Continuous Flow CCN counter, Aerosol Sci. Technol., 40, 242–254, 2006.
Lanz, V. A., Alfarra, M. R., Baltensperger, U., Buchmann, B., Hueglin, C., and Prevot, A. S. H.: Source Apportionment of Submicron Organic Aerosols at an Urban Site by Factor Analytical Modelling of Aerosol Mass Spectra, Atmos. Chem. Phys., 7, 1503–1522, 2007, http://www.atmos-chem-phys.net/7/1503/2007/.
Lee, S. H., Murphy, D. M., Thomson, D. S., and Middlebrook, A. M.: Chemical components of single particles measured with Particle Analysis by Laser Mass Spectrometry (PALMS) during the Atlanta SuperSite Project: Focus on organic/sulfate, lead, soot, and mineral particles, J. Geophys. Res., 107, 4003, doi:10.1029/2000JD000011, 2002.
Lee, S. H., Murphy, D. M., Thomson, D. S., and Middlebrook, A. M.: Nitrate and oxidized organic ions in single particle mass spectra during the 1999 Atlanta Supersite Project, J. Geophys. Res., 108, 8417, doi:10.1029/2001JD001455, 2003.

Lee, Y. S., Collins, D. R., Li, R. J., Bowman, K. P., and Feingold, G.: Expected impact of an aged biomass burning aerosol on cloud condensation nuclei and cloud droplet concentrations, J. Geophys. Res., 111, D22204, doi:10.1029/2005JD006464, 2006.

Liu, Y. G. and Daum, P. H.: Anthropogenic aerosols – Indirect warming effect from dispersion forcing, Nature, 419, 580–581, 2002.

Lough, G. C., Schauer, J. J., and Lawson, D. R.: Day-of-week trends in carbonaceous aerosol composition in the urban atmosphere, Atmos. Environ., 40, 4137–4149, 2006.

McFiggans, G., Alfarra, M. R., Allan, J., Bower, K. N., Coe, H., Cubison, M., Topping, D., Williams, P. I., Decesari, S., Facchini, C., and Fuzzi, S.: Simplification of the representation of the organic component of atmospheric particulates., Faraday Discuss., 130, 341–362, doi:10.1039/b419435g, 2005.

McMurry, P. H., Litchy, M., Huang, P.-F., Cai, X., Turpin, B. J., Dick, W. D., and Hanson, A.: Elemental composition and morphology of individual particles separated by size and hygroscopicity with the TDMA, Atmos. Environ., 30, 101–108, 1996.

McMurry, P. H., Wang, X., Park, K., and Ehara, E.: The Relationship Between Mass and Mobility for Atmospheric Particles: A New Technique for Measuring Particle Density., Aerosol Sci. Technol., 36, 227–238, 2002.

Medina, J., Nenes, A., Sotiropoulou, R. E. P., Cottrell, L. D., Ziemba, L. D., Beckman, P. J., and Griffin, R. J.: Cloud Condensation Nuclei (CCN) closure during the ICARTT 2004 campaign: a) effects of size-resolved composition, J. Geophys. Res., 112, D10S31, doi:10.1029/2006JD007588, 2007.

Middlebrook, A., Murphy, D. M., Lee, S.-H., Thomson, D. S., Prather, K. A., Wenzel, R. J., Liu, D.-Y., Phares, D. J., Rhoads, K. P., Wexler, A. S., Johnston, M. V., Jimenez, J. L., Jayne, J. T., Worsnop, D. R., Yourshaw, I., Seinfeld, J. H., and Flagan, R. C.: A Comparison of Particle Mass Spectrometers During the 1999 Atlanta Supersite Project, J. Geophys. Res., 108, 8424, doi:10.1029/2001JD000660, 2003.

Mircea, M., Facchini, M. C., Decesari, S., Cavalli, F., Emblico, L., Fuzzi, S., Vestin, A., Rissler, J., Swietlicki, E., Frank, G., Andreae, M. O., Maenhaut, W., Rudich, Y., and Artaxo, P.: Importance of the organic aerosol fraction for modeling aerosol hygroscopic growth and activation: a case study in the Amazon Basin, Atmos. Chem. Phys., 5, 3111–3126, 2005, http://www.atmos-chem-phys.net/5/3111/2005/.

Mochida, M., Kuwata, M., Miyakawa, T., Takegawa, N., Kawamura, K., and Kondo, Y.: Relationship between hygroscopicity and cloud condensation nuclei activity for urban aerosols in

Tokyo., J. Geophys. Res., 111, D23204, doi:10.1029/2005JD006980, 2006.
Molina, L. T., Kolb, C. E., de Foy, B., Lamb, B. K., Brune, W. H., Jimenez, J. L., and Molina, M. J.: Air Quality in North America's Most Populous City – Overview of MCMA-2003 Campaign, Atmos. Chem. Phys. Discuss., 7, 3113–3177, 2007, http://www.atmos-chem-phys-discuss.net/7/3113/2007/.
Murphy, D. M., Cziczo, D. J., Froyd, K. D., Hudson, P. K., Matthew, B. M., Middlebrook, A. M., Peltier, R. E., Sullivan, A., Thomson, D. S., and Weber, R. J.: Single-particle mass spectrometry of tropospheric aerosol particles, J. Geophys. Res., 111, D23S32, doi:10.1029/2006JD007340, 2006.
Niemi, J. V., Saarikoski, S., Tervahattu, H., Makela, T., Hillamo, R., Vehkamaki, H., Sogacheva, L., and Kulmala, M.: Changes in background aerosol composition in Finland during polluted and clean periods studied by TEM/EDX individual particle analysis, Atmos. Chem. Phys., 6, 5049–5066, 2006, http://www.atmos-chem-phys.net/6/5049/2006/.
Noble, C. A. and Prather, K. A.: Real-time measurement of correlated size and composition profiles of individual atmospheric aerosol particles, Environ. Sci. Technol., 30, 2667–2680, 1996.
Petters, M. D., Prenni, A. J., Kreidenweis, S. M., DeMott, P. J., Matsunaga, A., Lim, Y. B., and Ziemann, P. J.: Chemical aging and the hydrophobic-to-hydrophilic conversion of carbonaceous aerosol, Geophys. Res. Lett., 33, L24806, doi:10.1029/2006GL027249, 2006.
Petters, M. D. and Kreidenweis, S.: A single parameter representation of hygroscopic growth and cloud condensation nucleus activity, Atmos. Chem. Phys., 7, 1961–1971, 2007, http://www.atmos-chem-phys.net/7/1961/2007/.
Prenni, A. J., Petters, M. D., Kreidenweis, S. M., DeMott, P. J., and Ziemann, P. J.: Cloud droplet activation of secondary organic aerosol, J. Geophys. Res., 112, D10223, doi:10.1029/2006JD007963, 2007.
Quinn, P. K., Bates, T. S., Coffman, D. J., and Covert, D. S.: Influence of particle size and chemistry on the cloud nucleating properties of aerosols, Atmos. Chem. Phys. Discuss., 7, 14 171–14 208, 2007.
Raymond, T. M. and Pandis, S. N.: Cloud activation of single-component organic aerosol particles, J. Geophys. Res., 107, 4787, doi:10.1029/2002JD002159, 2002.
Riemer, N., Vogel, H., and Vogel, B.: Soot aging time scales in polluted regions during day and night., Atmos. Chem. Phys., 4, 1885–1893, 2004,

http://www.atmos-chem-phys.net/4/1885/2004/.
Rissler, J., Swietlicki, E., Zhou, J., Roberts, G., Andreae, M. O., Gatti, L. V., and Artaxo, P.: Physical properties of the sub-micrometer aerosol over the Amazon rain forest during the wet-to-dry season transition – comparison of modeled and measured CCN concentrations, Atmos. Chem. Phys., 4, 2119–2143, 2004, http://www.atmos-chem-phys.net/4/2119/2004/.
Roberts, G., Mauger, G., Hadley, O., and Ramanathan, V.: North American and Asian aerosols over the eastern Pacific Ocean and their role in regulating cloud condensation nuclei, J. Geophys. Res., 111, D13205, doi:10.1029/2005JD006661., 2006.
Roberts, G. C., Artaxo, P., Zhou, J. C., Swietlicki, E., and Andreae, M. O.: Sensitivity of CCN spectra on chemical and physical properties of aerosol: A case study from the Amazon Basin, J. Geophys. Res., 107, 8070, doi:10.1029/2001JD000583, 2002.
Roberts, G. C., Nenes, A., Seinfeld, J. H., and Andreae, M. O.: Impact of biomass burning on cloud properties in the Amazon Basin, J. Geophys. Res., 108, 4062, doi:10.1029/2001JD000985, 2003.
Roberts, G. C. and Nenes, A.: A continuous-flow streamwise thermal-gradient CCN chamber for atmospheric measurements, Aerosol Sci. Technol., 39, 206–221, 2005.
Ruehl, C. R., Chuang, P. Y., and Nenes, A.: How quickly do cloud droplets from on atmospheric particles?, Atmos. Chem. Phys. Discuss., 7, 14 233–14 264, 2007.
Salcedo, D., Onasch, T. B., Dzepina, K., Canagaratna, M. R., Zhang, Q., Huffman, J. A., DeCarlo, P. F., Jayne, J. T., Mortimer, P., Worsnop, D. R., Kolb, C. E., Johnson, K. S., Zuberi, B., Marr, L. C., Volkamer, R., Molina, L. T., Molina, M. J., Cardenas, B., Bernabe, R. M., Marquez, C., Gaffney, J. S., Marley, N. A., Laskin, A., Shutthanandan, V., Xie, Y., Brune, W., Lesher, R., Shirley, T., and Jimenez, J. L.: Characterization of ambient aerosols in Mexico City during the MCMA-2003 campaign with Aerosol Mass Spectrometry: results from the CENICA Supersite, Atmos. Chem. Phys., 6, 925–946, 2006, http://www.atmos-chem-phys.net/6/925/2006/.
Slowik, J. G., Stainken, K., Davidovits, P., Williams, L. R., Jayne, J. T., Kolb, C. E., Worsnop, D. R., Rudich, Y., DeCarlo, P. F., and Jimenez, J. L.: Particle morphology and density characterization by combined mobility and aerodynamic diameter measurements, Part 2: Application to combustion-generated soot aerosols as a function of fuel equivalence ratio, Aerosol Sci. Technol., 38, 1206–1222, 2004.
Sotiropoulou, R. E. P., Medina, J., and Nenes, A.: CCN predictions: Is theory suf-

ficient for assessments of the indirect effect?, Geophys. Res. Lett., 33, L05816, doi:10.1029/2005GL025148, 2006.
Sotiropoulou, R. E. P., Nenes, A., Adams, P. J., and Seinfeld, J. H.: Cloud condensation nuclei prediction error from application of Kohler theory: Importance for the aerosol indirect effect, J. Geophys. Res., 112, D12202, doi:10.1029/2006JD007834, 2007.
Spencer, M. T., Shields, L. G., and Prather, K. A.: Simultaneous Measurement of the Effective Density and Chemical Composition of Ambient Aerosol Particles, Environ. Sci. Technol., 41, 1303–1309, doi:10.1021/es061425+, 2007.
Stroud, C. A., Nenes, A., Jimenez, J. L., DeCarlo, P., Huffman, J. A., Bruintjes, R., Nemitz, E., Delia, A. E., Toohey, D. W., Guenther, A. B., and Nandi, S.: Cloud Activating Properties of Aerosol Observed during CELTIC, J. Atmos. Sci., 64, 441–459, 2007.
Svenningsson, I. B., Hansson, H. C., Wiedensohler, A., Ogren, J., Noone, K. J., and Hallberg, A.: Hygroscopic Growth of Aerosol-Particles in the Po Valley, Tellus, 44B, 556–569, 1992.
Swietlicki, E., Zhou, J., Berg, O. H., Martinsson, B. G., Frank, G., Cederfelt, S., Dusek, U., Berner, A., Birmili, W., Wiedensohler, A., Yuskiewicz, B., and Bower, K. N.: A closure study of sub-micrometer aerosol particle hygroscopic behaviour, Atmos. Res., 50, 205–240, 1999.
Textor, C., Schulz, M., Guibert, S., Kinne, S., Balkanski, Y., Bauer, S., Berntsen, T., Berglen, T., Boucher, O., Chin, M., Dentener, F., Diehl, T., Easter, R., Feichter, H., Fillmore, D., Ghan, S., Ginoux, P., Gong, S., Kristjansson, J. E., Krol, M., Lauer, A., Lamarque, J. F., Liu, X., Montanaro, V., Myhre, G., Penner, J., Pitari, G., Reddy, S., Seland, O., Stier, P., Takemura, T., and Tie, X.: Analysis and quantification of the diversities of aerosol life cycles within AeroCom, Atmos. Chem. Phys., 6, 1777–1813, 2006, http://www.atmos-chem-phys.net/6/1777/2006/.
Tolocka, M. P., Lake, D. A., Johnston, M. V., and Wexler, A. S.: Size-resolved fine and ultrafine particle composition in Baltimore, Maryland, J. Geophys. Res., 110, D07S04, doi:10.1029/2004JD004573, 2005.
Twomey, S.: Pollution and planetary albedo, Atmos. Environ., 8, 1251–1256, 1974.
Twomey, S.: Aerosols, Clouds and Radiation, Atmos Environ., 25, 2435–2442, 1991.
Twomey, S. A.: The influence of pollution on the shortwave albedo of clouds., J. Atmos. Sci., 34, 1148–1152, 1977.
Ulbrich, I.: Source apportionment of AMS data in Pittsburgh, Mexico City, and Houston by PMF, Eos Trans. AGU, 87, Fall Meet. Suppl., Abstract A23C-0980, 2006.
VanReken, T. M., Rissman, T. A., Roberts, G. C., Varutbangkul, V., Jonsson, H. H., Flagan,

R. C., and Seinfeld, J. H.: Toward aerosol/cloud condensation nuclei (CCN) closure during CRYSTAL-FACE, J. Geophys. Res., 108, 4633, doi:10.1029/2003JD003582, 2003.

VanReken, T. M., Ng, N. L., Flagan, R. C., and Seinfeld, J. H.: Cloud condensation nucleus activation properties of biogenic secondary organic aerosol, J. Geophys. Res., 110, D07206, doi:10.1029/2004JD005465, 2005.

Varutbangkul, V., Brechtel, F. J., Bahreini, R., Ng, N. L., Keywood, M. D., Kroll, J. H., Flagan, R. C., Seinfeld, J. H., Lee, A., and Goldstein, A. H.: Hygroscopicity of secondary organic aerosols formed by oxidation of cycloalkenes, monoterpenes, sesquiterpenes, and related compounds, Atmos. Chem. Phys., 6, 2367–2388, 2006, http://www.atmos-chem-phys.net/6/2367/2006/.

Volkamer, R., Jimenez, J. L., Martini, F. S., Dzepina, K., Zhang, Q., Salcedo, D., Molina, L. T., Worsnop, D. R., and Molina., M. J.: Secondary Organic Aerosol Formation from Anthropogenic Air Pollution: Rapid and Higher than Expected., Geophys. Res. Lett., 33, L17811, doi:10.1029/2006GL026899, 2006.

Wang, J. and Martin, S. T.: Satellite characterization of urban aerosols: Importance of including hygroscopicity and mixing state in the retrieval algorithms, J. Geophys. Res., 112, D17203, doi:10.1029/2006JD008078, 2007.

Warner, J.: Microstructure of Cumulus Cloud, 2. Effect on Droplet Size Distribution of Cloud Nucleus Spectrum and Updraft Velocity, J. Atmos. Sci., 26, 1272–1282, 1969.

Weingartner, E., Burtscher, H., and Baltensperger, U.: Hygroscopic properties of carbon and diesel soot particles, Atmos. Environ., 31, 2311–2327, 1997.

Zhang, Q., Stanier, C. O., Canagaratna, M. C., Jayne, J. T., Worsnop, D. R., Pandis, S. N., and Jimenez, J. L.: Insights into the Chemistry of New Particle Formation and Growth Events in Pittsburgh Based on Aerosol Mass Spectrometry, Environ. Sci Technol., 38, 4797–4809, 2004.

Zhang, Q., Alfarra, M. R., Worsnop, D. R., Allan, J. D., Coe, H., Canagaratna, M. R., and Jimenez, J. L.: Deconvolution and Quantification of Hydrocarbon-Like and Oxygenated Organic Aerosols Based on Aerosol Mass Spectrometry., Environ. Sci. Technol., 39, 4938–4952, 2005a.

Zhang, Q., Canagaratna, M. R., Jayne, J. T., Worsnop, D. R., and Jimenez, J. L.: Time and Size-Resolved Chemical Composition of Submicron Particles in Pittsburgh – Implications for Aerosol Sources and Processes, J. Geophys. Res., 110, D07S09, doi:10.1029/2004JD004649, 2005b.

Zhang, Q., Worsnop, D. R., Canagaratna, M. R., and Jimenez, J. L.: Hydrocarbon-like and oxygenated organic aerosols in Pittsburgh: insights into sources and processes of organic aerosols, Atmos. Chem. Phys., 5, 3289–3311, 2005c, http://www.atmos-chem-phys.net/5/3289/2005/.

Zhang, Q., Jimenez, J. L., Canagaratna, M. R., Allan, J. D., Coe, H., Ulbrich, I., Alfarra, M. R., Takami, A., Middlebrook, A. M., Sun, Y. L., Dzepina, K., Dunlea, E., Docherty, K., DeCarlo, P. F., Salcedo, D., Onasch, T., Jayne, J. T., Miyoshi, T., Shimono, A., Hatakeyama, S., Takegawa, N., Kondo, Y., Schneider, J., Drewnick, F., Weimer, S., Demerjian, K., Williams, P., Bower, K., Bahreini, R., Cottrell, L., Griffin, R. J., Rautiainen, J., and Worsnop., D. R.: Ubiquity and Dominance of Oxygenated Species in Organic Aerosols in Anthropogenically – Influenced Northern Hemisphere Mid-latitudes, Geophys. Res. Lett., 34, L13801, doi:10.1029/2007GL029979, 2007.

Table 1. Summary of the different models used in the CCN predictions. Note that in models 4 and 5, some of the hydrocarbon-like organic aerosol (HOA) is incorporated in the small-mode organics (SMO), see Fig. 4 for more detail. Estimated elemental carbon is treated as an additional externally-mixed and non-activating component in C3–5.

		State of mixing, with respect to the large-mode inorganics κ=0.5		
Model Case	Size-Resolved Composition?	Large-Mode Org. (LMO)	Small-Mode Org. (SMO)	Hydrocarbon-Like Organics (HOA)
1	No		Internal, κ=0.01	
2	Yes		External, Non-Activating	
3	Yes		Internal, κ=0.01	
4	Yes	Internal, κ=0.01	External, Non-Actv	Internal, κ=0.01*
5	Yes	Internal, κ=0.01	Internal, κ=0.01^{+}	External, Non-Actv

* If not part of SMO.
$^{+}$ If not part of the HOA.

CC BY

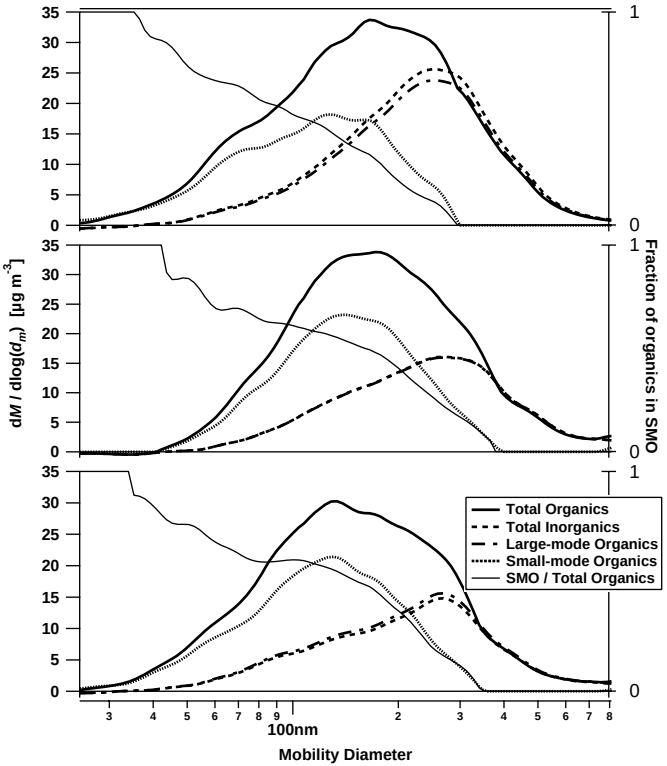

Fig. 1. Size resolved mass loadings from the AMS averaged for weekdays over the periods 06:00–07:00 (top), 12:00–13:00 (center) and 18:00–19:00 (bottom) h. The relative fractions of the inorganics to organics in the large-diameter internally-mixed mode are used to determine the assumed externally-mixed small mode organics. A more thorough explanation is given in the text. The size-resolved fraction of the organics calculated in the SMO is also shown. Although this does not change much over the diurnal cycle, there is more mass at the smaller diameters during the morning rush-hour period.

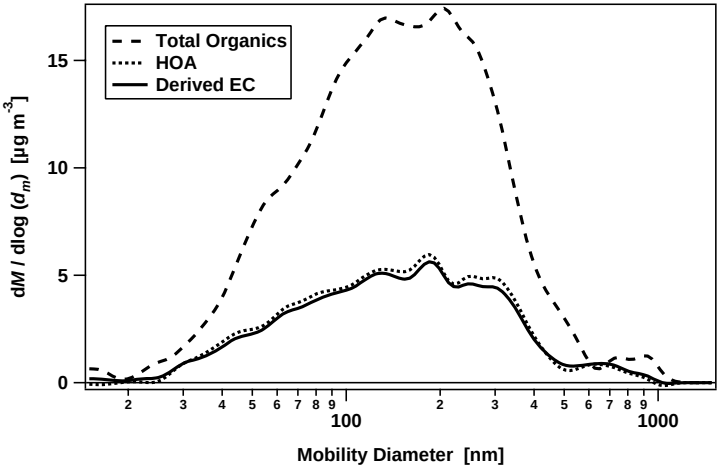

Fig. 2. Size-resolved mass loadings of the organics, Hydrocarbon-Like Organic Aerosol (HOA) and derived elemental carbon (EC, see methodology in text) for a weekday average from 06:00 to 07:00 h.

ACPD
8, 5629–5681, 2008

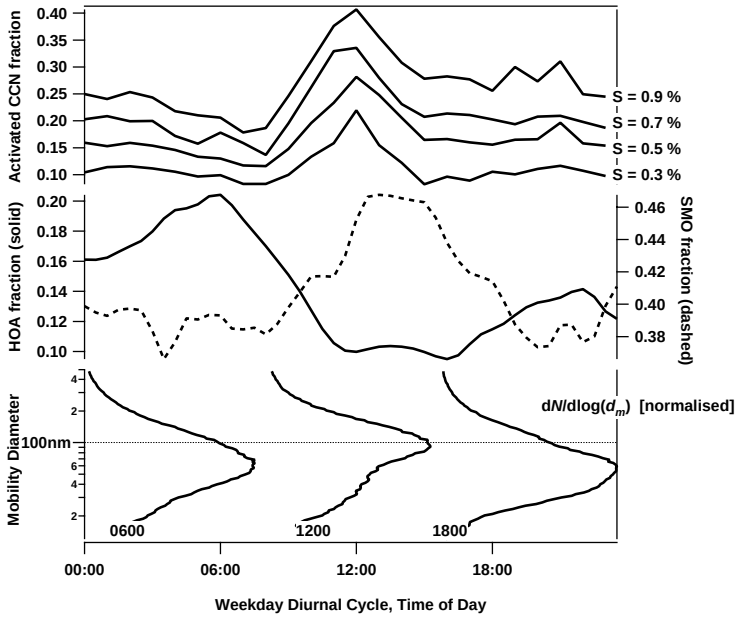

Fig. 3. Weekday diurnal cycles in the CCN activation, composition and size distribution during the SOAR-1 study. A clear cycle is observed in the CCN fraction, with the lowest value corresponding the to morning rush-hour. The variability in the CCN cycle corresponds both with variations in the aerosol composition, which exhibits the highest hydrocarbon-like organic aerosol fraction during the rush-hour, and with the size distribution, which grows to larger diameters during the peak in CCN activation. The fraction of the aerosol mass in the small organic mode does not vary greatly over the diurnal cycle.

ACPD
8, 5629–5681, 2008

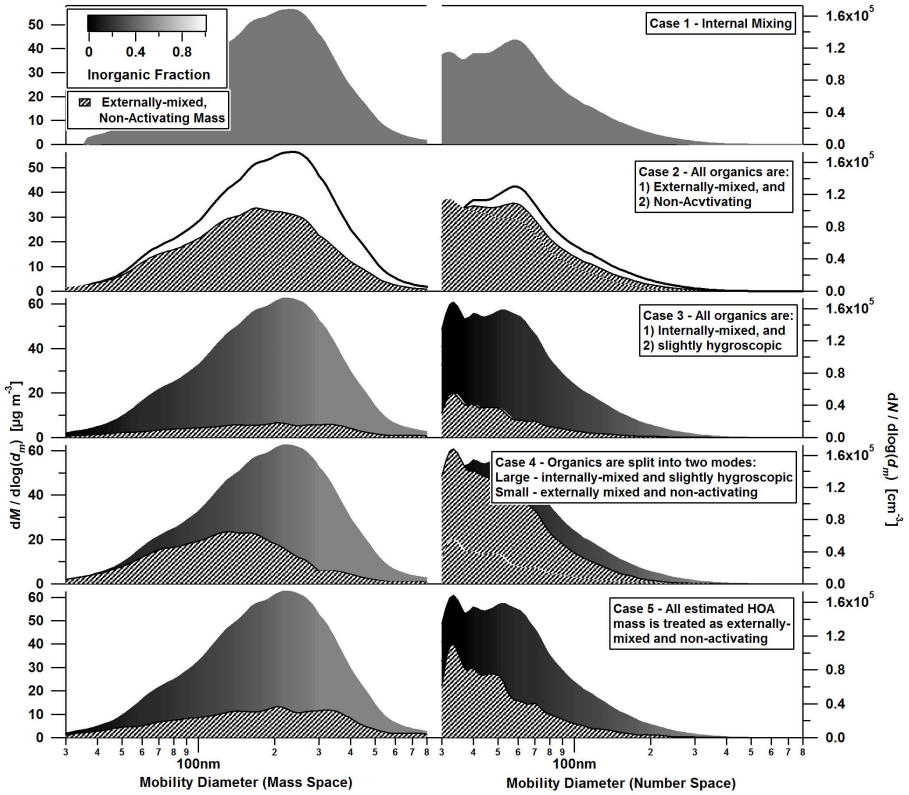

Fig. 4. Size-resolved mass (left) and number (right) distributions for a weekday average from 06:00 to 07:00 h showing the different modal inputs used in the various model cases C1 to C5.

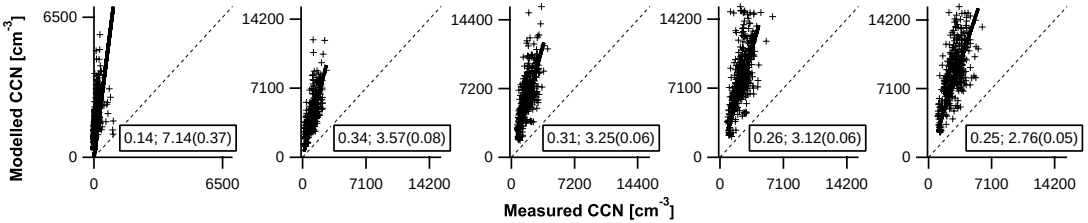

Fig. 5. Comparison of the predicted and measured CCN for the internal mixing case C1 at S=0.1, 0.3, 0.5, 0.7 and 0.9%; the R^2 value (left) and slope (with standard deviation in brackets) of a linear regression through the origin (right) are shown on each plot, and the regression line is overlaid on the measurements. Treating the population as completely internally-mixed leads to the model significantly over-predicting the CCN activation at all S.

ACPD
8, 5629–5681, 2008

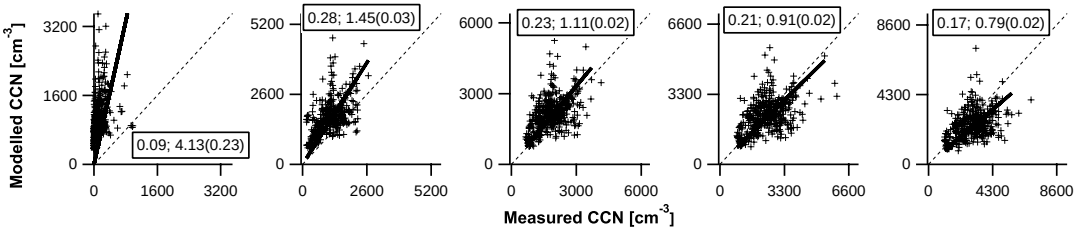

Fig. 6. Comparison of the predicted and measured CCN using the measured size resolved chemical composition where the distribution is treated as an external mixture of either purely inorganic or non-activating particles (C2), at S=0.1,0.3,0.5,0.7 and 0.9%. The R^2 value (left) and slope (with standard deviation in brackets) of the regression line forced through the origin (right) are shown on each plot, and the regression line is overlaid on the measurements.

ACPD
8, 5629–5681, 2008

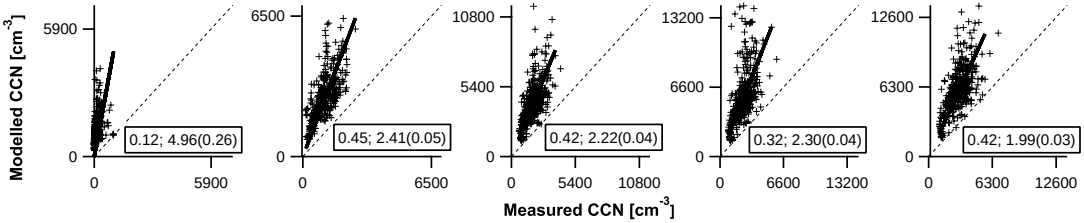

Fig. 7. Comparison of the predicted and measured CCN using the measured size resolved chemical composition with complete internal mixing of the inorganic and organic mass at each size, but treating the estimated elemental carbon as externally-mixed and entirely non-activating (C3), at S=0.1,0.3,0.5,0.7 and 0.9%. The R^2 value (left) and slope (with standard deviation in brackets) of the regression line forced through the origin (right) are shown on each plot, and the regression line is overlaid on the measurements. Although the smaller particles are now treated as organic-dominated, the model still over-predicts the CCN activation.

ACPD
8, 5629–5681, 2008

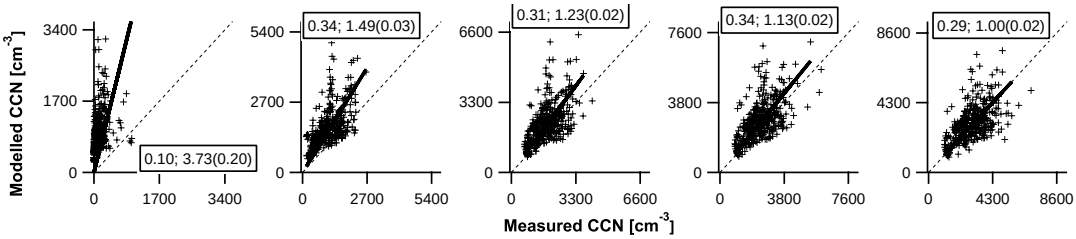

Fig. 8. Comparison of the predicted and measured CCN using the measured size resolved chemical composition where the small mode organics and estimated elemental carbon are treated as externally-mixed and entirely non-activating (C4), at S=0.1,0.3,0.5,0.7 and 0.9%. The R^2 value (left) and slope (with standard deviation in brackets) of the regression line forced through the origin (right) are shown on each plot, and the regression line is overlaid on the measurements. By assuming all the small mode organics are completely hydrophobic, the model now reaches reasonable agreement with the measurements on CCN activation.

ACPD
8, 5629–5681, 2008

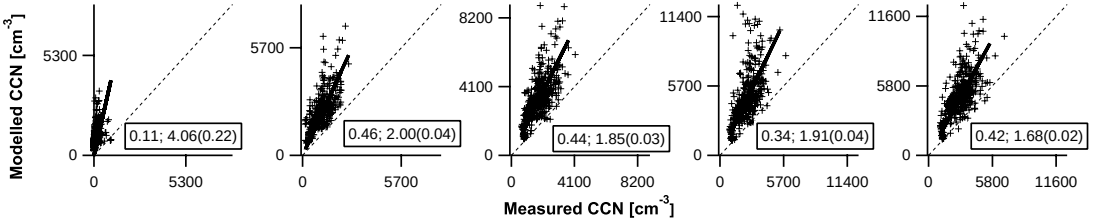

Fig. 9. Comparison of the predicted and measured CCN using the measured size resolved chemical composition where the hydrocarbon-like organic aerosol (HOA) and estimated elemental carbon (EC) are treated as externally-mixed and entirely non-activating, at S=0.1,0.3,0.5,0.7 and 0.9% (C5). The R^2 value (left) and slope (with standard deviation in brackets) of the regression line forced through the origin (right) are shown on each plot, and the regression line is overlaid on the measurements.

ACPD
8, 5629–5681, 2008

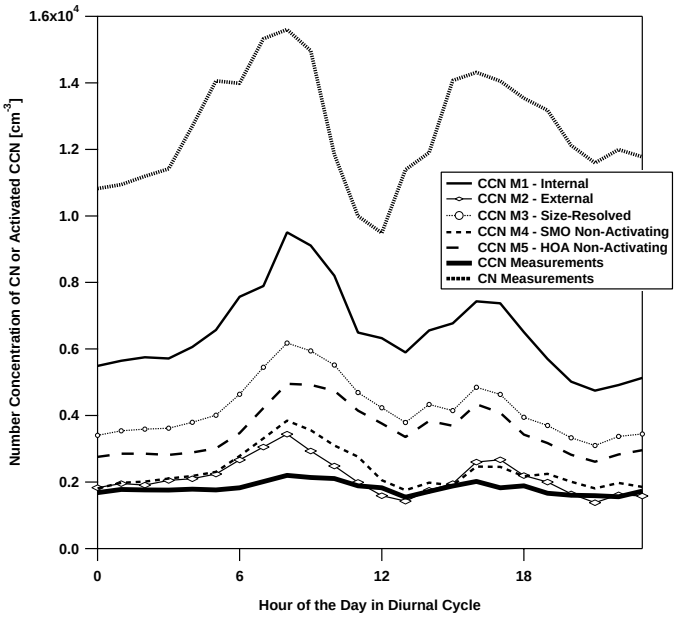

Fig. 10. Summary of the weekday diurnal cycles in CCN activation predicted by the five models and measured by the CCN counter at S=0.5%, together with the weekday diurnal cycle observed in the aerosol condensation nucleus (CN) measurements. All the models over-predict the measured CCN during the morning rush-hour period.

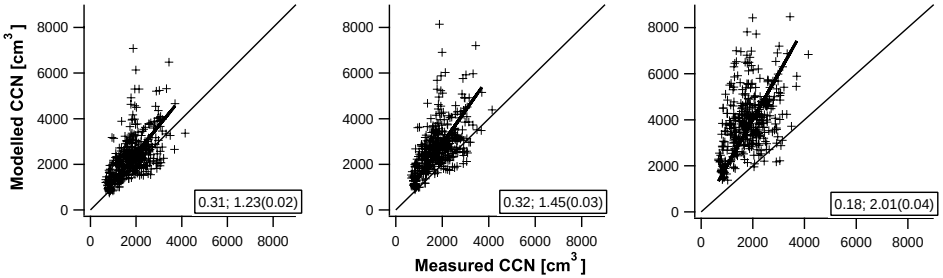

Fig. 11. Comparison of the predicted and measured CCN using CCN model case 4 (of Fig. 8) at S=0.5%; the reference case from Fig. 8 is shown on the left. Centre and right use the same model where the organics have κ values of 0.13 and 0.5. The R^2 value (left) and slope (with standard deviation in brackets) of the regression line forced through the origin (right) are shown on each plot, and the regression line is overlaid on the measurements. Increasing the hygroscopicity of the organics raises the predicted CCN in the model.

ACPD
8, 5629–5681, 2008

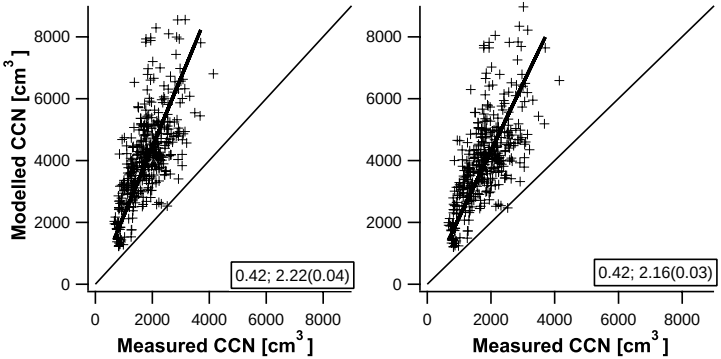

Fig. 12. Comparison of the predicted and measured CCN using CCN model case 3 (of Fig. 7) at S=0.5%; the reference case from Fig. 7 is shown on the left. The plot on the right uses the same model where the organics have a κ value approaching zero. The R^2 value (left) and slope (with standard deviation in brackets) of the regression line forced through the origin (right) are shown on each plot, and the regression line is overlaid on the measurements. Further decreasing the hygroscopicity of the organics in the model does not significantly decrease the predicted CCN concentration.

ACPD
8, 5629–5681, 2008

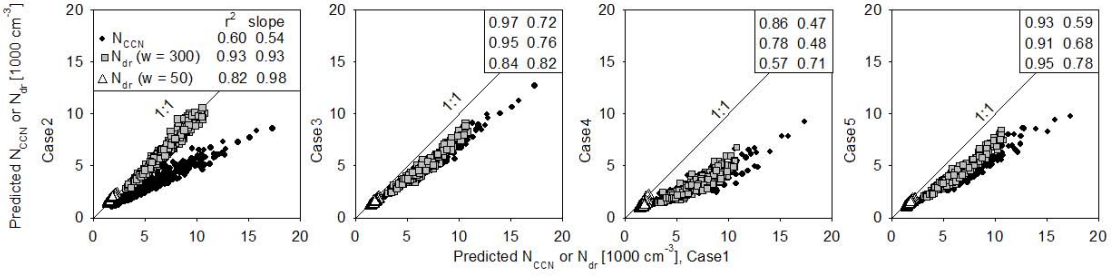

Fig. 13. Predicted CCN numbers and cloud droplet numbers (for two different updraft velocities) using the different model cases. The numbers in the upper right corner are the R^2 and slopes of the regression lines.

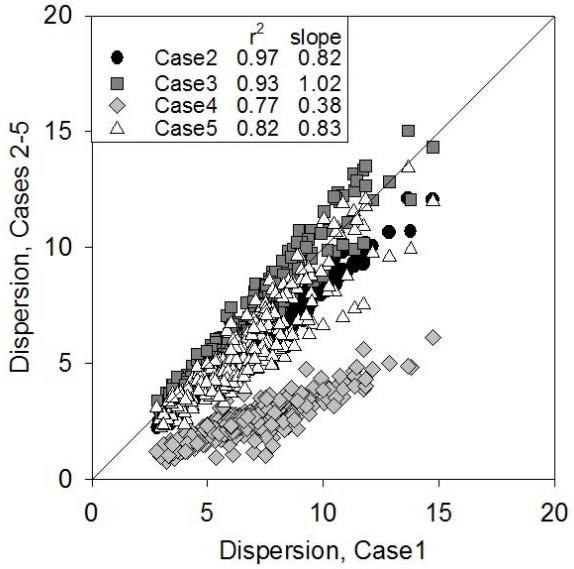

Fig. 14. Comparison of dispersion of cloud droplet size distribution at liquid water content 0.3 g m^{-3} (w=50 cm s^{-1}) for model cases 2, 3, 4, and 5 vs. C1 (see text).

ACPD
8, 5629–5681, 2008

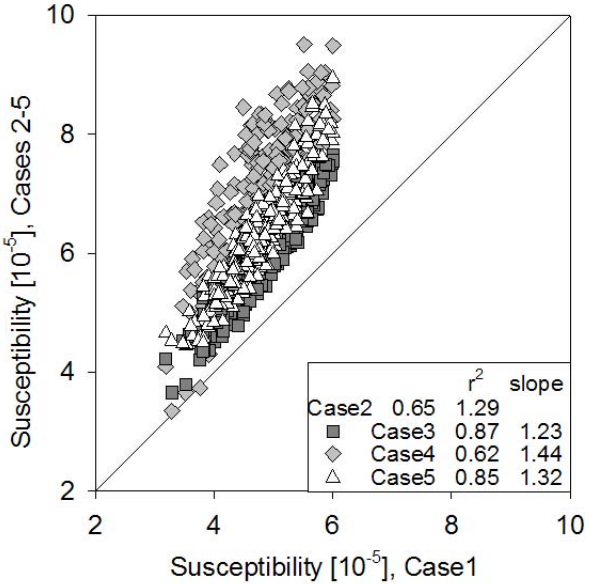

Fig. 15. Comparison of cloud susceptibility (Eq. (2)) at liquid water content 0.3 g m^{-3} (w=50 cm s^{-1}) for model cases 2, 3, 4, and 5 vs. C1 (see text).